(19) Europäisches Patentamt
European Patent Office
Office européen des brevets

(11) **EP 4 505 893 A1**

(12) **EUROPEAN PATENT APPLICATION**

(43) Date of publication:
12.02.2025 Bulletin 2025/07

(21) Application number: **23190882.3**

(22) Date of filing: **10.08.2023**

(51) International Patent Classification (IPC):
A41D 1/084 *(2018.01)* ***A41H 1/02*** *(2006.01)*

(52) Cooperative Patent Classification (CPC):
A41D 1/084; A41H 1/02; A41D 2600/104

(84) Designated Contracting States:
AL AT BE BG CH CY CZ DE DK EE ES FI FR GB GR HR HU IE IS IT LI LT LU LV MC ME MK MT NL NO PL PT RO RS SE SI SK SM TR
Designated Extension States:
BA
Designated Validation States:
KH MA MD TN

(71) Applicants:
- **SHER srl**
  39100 Bozen (IT)
- **Technische Universität München**
  80333 München (DE)

(72) Inventors:
- **Canali, Sara**
  39100 Bozen (IT)
- **Kati, Nispel**
  80333 München (DE)
- **Prof. Dr.-Ing. Veit, Senner**
  80333 München (DE)

(74) Representative: **DTS Patent- und Rechtsanwälte PartmbB**
Brienner Straße 1
80333 München (DE)

(54) PROTECTIVE PAD FOR A CYCLING GARMENT AND METHOD OF MANUFACTURING THE SAME

(57) The invention provides protective pad 100 for a cycling garment, said pad 100 including a 3D-printed body 10 made of a lattice structure 12, wherein said lattice structure 12 comprises different regions characterized by at least one different mechanical property. The invention further provides a cycling garment including the pad 100, a method of manufacturing the protective pad 100, a method measuring pressure distribution at the human-saddle interface on a static cycle, and a measurement saddle for use in this method.

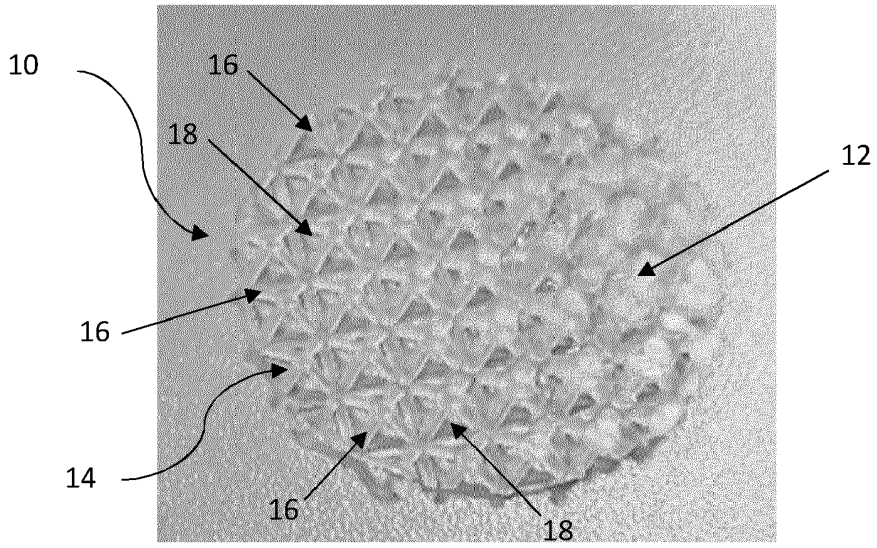

Fig. 1

EP 4 505 893 A1

Description

[0001] The present invention belongs to the technical field of protective pads for use in cycling garments to provide protection against pain and/or injuries and/or discomfort in the pelvic and/or genital area of a cyclist, e.g. a professional athlete, during training or racing.

[0002] For instance, said cycling garment may include cycling shorts, a cycling suit or a triathlon suit.

[0003] In particular, the present invention relates to an improved protective pad for a cycling garment, able to effectively prevent the risk of pain and/or injuries and/or discomfort in the pelvic and/or genital area during riding, and a cycling garment including the same.

[0004] Also, the present invention concerns a method for measuring pressure distribution at a saddle-human interface in a riding position, in particular for obtaining data regarding individual load patterns at the human-saddle interface for one or more subjects.

[0005] Also, the present invention concerns an improved measurement saddle for use in the above-mentioned method.

[0006] Finally, the invention concerns a method of manufacturing the above-mentioned protective pad, in particular based on the data regarding individual load patterns at the human-saddle interface obtained through the above-specified method.

[0007] Over the last few decades, cycling has become a popular sport and its positive effect on health and cardiorespiratory fitness has been widely demonstrated **[1].**

[0008] However, cyclists may encounter some health risks, in particular in terms of pain, injuries or other discomfort in the pelvic or genital area.

[0009] Especially with longer riding times (as in the case of professional athletes), a significant proportion of cyclists feel discomfort in the pelvic and/or genital area, such as numbness and irritation. Some of them also suffer from sexual dysfunction or chronic lymphedema, which in the worst cases may require surgical intervention.

[0010] In addition to friction and moisture, these complaints are mainly caused by unphysiological load on the pelvic and/or genital area while riding.

[0011] The potential health risks for cyclists, e.g. road cyclists, in particular professional athletes, have been widely investigated.

[0012] In particular, several studies have been carried out overtime considering the effects of cycling, in particular road cycling, on the reproductive system and the genitals.

[0013] The majority of these studies are focused on cycling-related issues in male athletes.

[0014] On the other hand, research concerning cycling-related issues in female athletes has been much less frequent.

[0015] Nonetheless, the risk of pain and/or injuries and/or discomfort in the pelvic and/or genital area equally concerns both female and male cyclists, especially in case of professional athletes.

[0016] A study revealed that the percentage of serious female cyclists, in particular road cyclists, suffering from pain and numbness in the genital area is larger than in swimmers or runners **[2].**

[0017] In the present context, with the definition "serious cyclist" it is intended a competitive athlete (either professional or non-professional) or, at least, an experienced athlete with a minimum of one cycling tour of at least 1.5 hours per week.

[0018] Another study revealed that around 40% of female road cyclists suffer from sitting discomfort in the crotch area **[3].**

[0019] Yet another study revealed that 30-40% of female cyclists experience genital numbness and sensory dysfunctions **[4],** which also correlates with decreased arousal and orgasm **[5], [6].**

[0020] In competitive cycling, the number of athletes reporting numbness or genital pain increases towards 63% **[7].**

[0021] Both in male and female athletes, pain and/or injuries and/or discomfort in the pelvic and/or genital area seem to largely depend on pressure loads at the human-saddle interface.

[0022] For this reason, pressure distributions at the human-saddle interface have been the focus of several studies **[8]-[10].**

[0023] The interface region between the saddle and the athlete can be divided into anterior and posterior regions defined along the longitudinal axis, as well as left and right regions defined along the mediolateral axis. In particular, the pressure configuration on the saddle shows three regions of intense load: one on the anteroposterior axis in the anterior region of the saddle, caused by the perineum and/or the genitals, the second and third in the posterior region of the saddle, respectively on the left and right side of the anteroposterior axis, caused by the ischial tuberosities **[11]-[14].**

[0024] Potter et al. revealed that men's and women's saddle pressure distributions are different for anatomical reasons **[11].**

[0025] Here, studies have been carried out with a pressure measurement mat while subjects pedaled at 100W and 200W. For the involved 11 female subjects, the center of pressure was on average further to the rear than for the involved 11 male athletes. As in male athletes, the pressure distribution in female athletes also varied depending on the seating position. In particular, when increasing the inclination angle of the upper body, a loading shift from posterior to anterior, as well as a decreasing distance between the posterior pressure centers could be observed. With an increased inclination

angle, the pressure distribution becomes more punctual. Potter et al. explain this as being due to the anterolaterally expanding pubic ramus of the female hip bone, which increasingly loses contact with the narrowed saddle with an increased upper body inclination angle **[11].**

[0026] This suggests that a differentiated protection for male and female cyclists could be desirable in order to more effectively prevent the occurrence of pain and/or injuries and/or discomfort in the pelvic and/or genital area.

[0027] Sauer et al. found that the anterior pelvic tilt in female cyclists is greater than for males, which is in line with the generally more anterior saddle loading in females **[15].**

[0028] In contrast, Carpes et al. **[16]** found no differences in pressure values when comparing an upright trunk position with an inclined trunk position in female athletes.

[0029] Anatomically, the skin in the female genital area is thinner and mechanically less resistant than normal skin **[17].**

[0030] Also, the additional fat tissue and the weak connective tissue on the outer side of the labia can foster infections and edematous swellings **[17].**

[0031] Moreover, Leibovitch et al. **[18]** suspect that, both in male and female cyclists, the nerves and blood flow under the outer organs are affected as a result of pressure at the human-saddle interface, which can again lead to numbness and other dysfunctions **[19].**

[0032] Different saddle designs and geometries, e.g. presence/absence of a cutout in the perineal region, presence/absence of cushioning and/or cushioning level, may have a significant impact on the risk of pain and/or injuries and/or discomfort for the athlete.

[0033] However, this aspect is highly subjective and greatly varies depending on the anatomy and/or preferences of the individual.

[0034] The positive effects of saddle design and geometry remain controversially discussed in the literature.

[0035] While Taylor et al. **[8]** and Sommer et al. **[9]** found that saddles with central cutouts improved comfort, to the contrary Partin et al. **[10]** contradicted these findings.

[0036] Noseless saddles are found to reduce pressure in the anterior pubis, but, unfortunately, do not provide sufficient support for the rider from a stability point of view **[20]-[22].**

[0037] Overall, no study was able to identify a significant correlation between saddle design and geometry and the occurrence of sexual dysfunction and/or genital pressure **[10], [21], [23], [24].**

[0038] Specific cycling garments, such as shorts or suits, provided with a protective pad have proven effective in reducing pressure at the human-saddle interface **[25],** thereby improving the overall comfort conditions for the cyclist **[25].**

[0039] Besides, these padded garments also show positive effects on moisture and temperature **[27]** and friction reduction due to seamless designs **[28].**

[0040] Padded garments, e.g. shorts or suits, therefore introduce another important variable worth of further investigation.

[0041] In Larsen et al. the sensory manifestations of a non-conservative pad design were investigated. In this experiment, the anterior height in cycling short padding was decreased by reducing the foam material thickness in the genital area by more than 60%. The study revealed that participants with a reduced pad were more likely to experience numbness and pain in the crotch area **[3].**

[0042] However, it has to be considered that athletes respond very differently to distinct solutions.

[0043] The wide majority of padded cycling garments include a unisex protective pad. That is, the pad design does not consider differences in anatomy between male and female cyclists.

[0044] Presently, there are only a few garments, mostly in the high-priced range, which are specifically adapted to the female anatomy.

[0045] Also, there are models of padded garments having a locally-adjusted stiffness in order to generate a more physiological load. This is mainly implemented by the use of gel inserts (e.g., W bike Bibshorts Hotbond produced by Löffler) or by the use of material inserts (e.g., UMA GTV Bib Shorts C2 or Gore Long Distance bib shorts + women produced by Assos) in the area of the sit bones.

[0046] Pressure distribution at the human-saddle interface varies significantly between cyclists.

[0047] In particular, pressure distribution may greatly vary depending on anatomy, mobility, posture and/or previous injuries of the cyclist.

[0048] Therefore, there is the need for a solution that provides for a proper individualization of pad design, allowing to effectively reduce the risk of pain and/or injuries and/or discomfort in the pelvic and/or genital area **[21], [25].**

[0049] In particular, there is a strongly-felt need for a solution that allows to provide an improved and more effective dampening in those areas where pressure load at the human-saddle interface is higher.

[0050] It is therefore an object of the present invention to provide an improved protective pad for a cycling garment, allowing to provide an enhanced and more effective protection against the risk of pain and/or injuries and/or other discomfort in the pelvic and/or genital area of a cyclist, in particular a female cyclist, more particularly a female road cyclist, while simultaneously improving the overall comfort conditions.

[0051] Another object of the present invention is to provide a cycling garment, such cycling shorts, a cycling suit or a

triathlon suit, including the above-mentioned pad.

[0052] Yet another object of the present invention is to provide a method for reliably measuring pressure distribution at the human-saddle interface.

[0053] Also, it is an object of the present invention to provide a measurement saddle for use in the above-mentioned method.

[0054] A still further object of the present invention is to provide a method of manufacturing a protective pad as defined above, in particular based on data regarding load patterns at the human-saddle interface obtained through the above-mentioned method.

[0055] The present invention concerns a protective pad for a cycling garment, said pad including a 3D-printed body made of a lattice structure, wherein said lattice structure comprises different regions characterized by at least one different mechanical property.

[0056] The present invention provides a protective pad for a cycling garment.

[0057] In particular, said protective pad includes a 3D-printed body made of a lattice structure.

[0058] In particular, said lattice structure comprises different regions characterized by at least one different mechanical property.

[0059] The invention is based on the basic idea that, by the provision of protective pad for a cycling garment including a lattice structure having different regions each characterised by different mechanical properties, it is possible to provide an improved and better-tuned protection, e.g. based on the anatomy of the cyclist and/or the effective pressure level at the human-saddle interface in each different region. Further, the use of a lattice structure offers a high degree of design freedom, allowing to locally adjust the mechanical properties of the protective pad. Also, said lattice structure may be easily obtained through additive manufacturing with reduced costs.

[0060] Advantageously, said mechanical property may include thickness.

[0061] Accordingly, it is possible to provide a lattice structure where two or more regions are characterised by different thicknesses, e.g. based on the effective pressure level at the human-saddle interface for each of said regions.

[0062] In particular, regions characterised by a higher pressure level (level with a higher pressure level than other regions of the pad) at the human-saddle interface may have an increased thickness, so as to provide an improved dampening effect.

[0063] Advantageously, the lattice structure may be a grid made of a plurality of grid cells, each including crossing beams defining a void therebetween.

[0064] This allows to prevent sweat from being retained within the structure, which may generate irritations and discomfort.

[0065] Accordingly, the overall comfort conditions for the cyclist during riding may be significantly improved.

[0066] Advantageously, grid cells defining regions of the lattice structure having a higher thickness may include beams which are larger in cross-section.

[0067] Similarly, grid cells defining regions of the lattice structure having a reduced thickness may include beams which are smaller in cross-section.

[0068] Otherwise stated, the thickness level in each region can be tuned by acting on the thickness of the beams forming each grid cell.

[0069] Advantageously, the regions of the lattice structure having a higher thickness may correspond to regions that are subject to a higher pressure load at the human-saddle interface in a riding position.

[0070] Similarly, the regions of the lattice structure having a reduced thickness correspond to regions that are subject to a lower pressure load at the human-saddle interface in a riding position.

[0071] The present invention also provides a cycling garment including the above-defined protective pad.

[0072] For instance, said garment can be cycling shorts.

[0073] Alternatively, said cycling garment can be a cycling suit.

[0074] As a further alternative, said cycling garment can be a triathlon suit.

[0075] Triathlon suits are similar to cycling suits, but usually include a narrower protective pad to allow the athlete to swim and run without having any discomfort connected to the presence of the protective pad.

[0076] Preferably, said cycling garment is specifically designed for the anatomy of a female cyclist.

[0077] Even more preferably, said cycling garment is specifically designed for the anatomy of a female road cyclist.

[0078] The present invention also relates to a method for measuring pressure distribution at the human-saddle interface on a static cycle.

[0079] The method includes the step of performing a cycle-fitting process while a participant is pedaling sitting on a saddle of the static cycle in a riding position, for adjusting at least a position, height and inclination of the saddle, a position of the handlebar and crank arm lengths.

[0080] Cycle-fitting processes are known in the art and are usually implemented to optimize bike settings based on the characteristics and/or preferences of the athlete.

[0081] This allows not only to improve the performance while riding, but also to prevent injuries, e.g. due to a sub-optimal

position on the bike while riding.

[0082] This even more applies in case of professional cyclists, usually spending a significant number of hours on the bike for both training and racing.

[0083] Usually, cycle-fitting processes may comprise the following steps:

- collecting data for the assessment of a participant both off the bike and on the bike, e.g. comprising one or more among:

  interviewing the participant to determine his/her riding position preferences, level of cycling, areas of discomfort or the like;

  collecting anthropometric data of the participant, both off the bike and while pedaling in the riding position of said participant. In particular, said anthropometric data can be collected in a standing position of said participant and/or while pedaling in the riding position of said participant, and

  measuring hip flexibility of the participant, e.g. through a goniometer;

- defining an optimal riding position based on the collected data, and

- providing optimized bike settings for the participant, e.g. comprising size of the bike frame and size/settings for those components of the bike that influence the riding position, e.g. the saddle, seat post, handlebars, and/or crank arm lengths.

[0084] For instance, the cycle-fitting process can be carried out by using an idmatch smart bike (idmatch, Selle Italia®, Casella d'Asolo, Italy).

[0085] According to the invention, the cycle-fitting process may advantageously comprise the following steps of:

collecting anthropometric data of said participant, in particular in a standing position of said participant and/or while pedaling in the riding position of said participant, and

implementing a real-time algorithm for defining optimized parameters for adjusting at least a position height and inclination of the saddle, a position of the handlebar and crank arm lengths, based at least on the collected anthropometric data of the participant.

[0086] The method further includes:

providing a measurement saddle;

layering a first amount of a plastically deformable material on a carrier structure of the measurement saddle;

providing a cover on said plastically deformable material, layered on the carrier structure of the measurement saddle;

replacing the saddle of the static cycle with the measurement saddle;

forming a first mold in a dynamic condition, while the participant is pedaling on the measurement saddle in the riding position;

removing the first mold from the measurement saddle;

layering a new amount of plastically deformable material on the carrier structure of the measurement saddle;

providing a cover on said plastically deformable material, layered on the carrier structure;

forming a second mold in a static condition, while the participant is sitting on the measurement saddle in the riding position with the crank arms of the static bike placed in a horizontal position;

removing the second mold from the measurement saddle;

performing a 3D scanning process of the first mold and the second mold;

superimposing the obtained 3D scans along a reference coordinate system, and implementing software means for generating a surface model of the superimposed 3D scans and obtaining data regarding individual load patterns at the human-saddle interface for the participant.

[0087] For example, said plastically deformable material can be soft plasticine.

[0088] In particular, the inventors have found that, in this context, soft plasticine provides the most appropriate deformation ranges as a molding mass.

[0089] Also, said plastically deformable material, e.g. soft plasticine, is suitable for re-use in multiple measurements thanks to its ability of deforming in a reversible manner without any change to its properties.

[0090] By implementing measurements both in dynamic and static positions, it is possible to define individual load patterns at the human-saddle interface with a high level of reliability.

[0091] The cycle-fitting process can be implemented while the participant is pedaling on the static cycle for 15 minutes at 60 rpm and 100W in the riding position.

[0092] The step of forming the first mold can be performed while the participant is pedaling on the static cycle for 20 minutes at 60 rpm and 100W in the riding position.

[0093] The step of forming the second mold can be performed while the participant is sitting on the measurement saddle in the riding position for 20 minutes, changing the left/right foot position after the first 10 minutes.

[0094] Preferably, said riding position is a position on the drops.

[0095] With "position on the drops" or "drops position", it is intended a position where the subject holds the handlebar of a bike, preferably a racing bike, maintaining his/her hands on the curved portion of said handlebar, behind the levers of the brake and the shift.

[0096] Alternatively, said riding position can be a position on the tops.

[0097] With "position on the tops", it is intended a position where the subject holds the handlebar of a bike, e.g. a mountain bike, maintaining his/her hands on the straight portion of said handlebar.

[0098] As a further alternative, said riding position can be a position for time-trial, where the cyclist has his/her hands holding aero bars.

[0099] Advantageously, the above-mentioned anthropometric data of the participant may include hip width.

[0100] Additionally or alternatively, said anthropometric data of the participant may include hip rotation angle.

[0101] Additionally or alternatively, said anthropometric data of the participant may include lumbar angle.

[0102] Preferably, said anthropometric data of the participant include a combination of hip width, hip rotation angle and lumbar angle.

[0103] This allows to obtain anthropometric data characterised by a high level of reliability.

[0104] Preferably, the hip rotation angle is measured in the sagittal plane between the thigh and lumbar spine alignment when performing a maximum possible forward bend.

[0105] Preferably, the lumbar spine angle is defined by the angle between the lumbar and thoracic spine orientation in the same forward bend.

[0106] Preferably, said anthropometric data of the participant are collected by using a depth-sensing camera.

[0107] This provides a simple way to perform anthropometric data collection with a high level of accuracy.

[0108] Advantageously, the definition of optimized parameters for adjusting at least a position, height and inclination of the saddle, a position of the handlebar, and crank arm lengths may be further based on a pain status of the participant.

[0109] Additionally or alternatively, the definition of optimized parameters for adjusting at least a position, height and inclination of the saddle, a position of the handlebar, and crank arm lengths may be further based on continuously measured joint angles.

[0110] By further considering a pain status of the participant and/or continuously measured joint angles, it is possible to define said optimised parameters with an improved level of accuracy.

[0111] The step of layering the plastically deformable material on the carrier structure of the measurement saddle may comprise providing a first layer and a second layer of said plastically deformable material, e.g. soft plasticine, on said carrier structure.

[0112] Preferably, each of said first and second layers has a height of 15 mm.

[0113] This allows to obtain a mold that reliably reflects pressure points at the human-saddle interface.

[0114] The method may further include the step of providing a mark on the obtained first mold and second mold, at a predefined location along the longitudinal axis of the carrier structure.

[0115] For instance, said mark may be carved in the mold.

[0116] The mark is used as a reference point in 3D-scanning and data analysis.

[0117] Advantageously, the 3D-scanning process may be carried out by placing each of the first and second molds on a rotary plate, after covering each of the first and second molds with a chalk spray.

[0118] Accordingly, a reliable 3D-scan of the first and second molds can be obtained.

[0119] The method may further comprise removing residual plastically deformable material protruding from the bottom

end of the first and second molds.

[0120] This can be performed, for instance, by using a knife.

[0121] Accordingly, said molds can be located in a planar position for 3D-scanning.

[0122] After replacement of the saddle of the static cycle with the measurement saddle, the method may further include dropping the seatpost of the static cycle of 15 mm.

[0123] This allows to achieve the position suggested by the cycle-fitting process, considering the height differences between the saddle of the static cycle bike and the measurement saddle.

[0124] The present invention further provides a method of manufacturing the above-described protective pad for a cycling garment.

[0125] In particular, the method comprises implementing the above-described method for measuring pressure distribution at the human-saddle interface on a static cycle for at least one participant.

[0126] This allows to obtain data regarding individual load patterns at the human-saddle interface for said at least one participant.

[0127] For instance, said participant can be a road cyclist, in particular a female road cyclist, as in the experimental study described below.

[0128] The method further comprises generating a digital mold model of the lattice structure, based on said data regarding individual load patterns at the human-saddle interface for the at least one participant.

[0129] Still further, the method comprises implementing a 3D-printing process for manufacturing the protective pad, based on the generated 3D model.

[0130] By manufacturing a protective pad for a cycling garment based on a 3D model that considers individual load patterns at the human-saddle interface, it is possible to obtain a cycling garment which is able to provide an improved protection against pain and/or injuries and/or discomfort in the pelvic and/or genital area, in particular by providing an enhanced dampening effect in those areas that are subject to higher pressure at the human-saddle interface in the riding position.

[0131] Advantageously, the protective pad may be specifically tailored on the characteristic load patterns of a single athlete, e.g. a female road cyclist, thereby providing an improved, highly-personalised protection.

[0132] Advantageously, the method may comprise implementing the above-described method for measuring pressure distribution at the human-saddle interface on a static cycle for a plurality of participants.

[0133] Accordingly, data regarding individual load patterns at the human-saddle interface can be obtained for each participant.

[0134] Here, the method further includes generating an average reference data set based on the obtained data regarding individual load patterns at the human-saddle interface for said plurality of participants.

[0135] The digital mold model of the lattice structure is generated based on said average reference data set.

[0136] Although not as specific as in the case of a protective pad that is tailored based on the individual load patterns at the human-saddle interface for a single participant, this solution still allows to provide an improved, well-tuned protection, in particular by providing an enhanced dampening in those regions that are subject to higher pressure load while riding.

[0137] This even more applies when the involved participants have similar anatomical characteristics.

[0138] For instance, said plurality of participants may include a plurality of female cyclists.

[0139] Preferably, said plurality of participants may include a plurality of female road cyclists, as in the experimental study described below.

[0140] Finally, the present invention provides a measurement saddle for use in the above-described method for measuring pressure distribution at the human-saddle interface.

[0141] The measurement saddle includes a carrier structure.

[0142] In particular, said carrier structure comprises a saddle-shaped base, acting as a level surface.

[0143] The carrier structure further includes a plurality of fixture parts.

[0144] In particular, said plurality of fixture parts is configured and adapted for acting as boundaries for a plastically deformable material to prevent undesired material flow.

[0145] Accordingly, when the plastically deformable material, e.g. soft plasticine, is layered on the saddle-shaped base, unwanted flow of said material can be largely prevented.

[0146] There is also a saddle rail, which allows to fit and secure the measurement saddle to an existing seatpost of a cycle, e.g. a smart bike.

[0147] The measurement saddle is suitable for use in quantitative measurements of the pressure distribution, where locally appearing pressure values are assumed to be proportional to the material displacement of the molding mass.

[0148] This approach has proven effective in order to allow a higher resolution of pressure distribution on the seating surface, and ensure accurate measurements independent of a specific, underlying saddle geometry.

[0149] In particular, the carrier structure may have a length of 250 mm and a maximum width of 210 mm.

[0150] In particular, said plurality of fixture parts may comprise a first fixture part and a second fixture part.

[0151] In particular, the first fixture part may be connected, e.g. screwed, to the anterior end of the saddle-shaped base.

[0152] In particular, the second fixture part may be connected, e.g. screwed, to the posterior end of the saddle-shaped base.

[0153] In particular, said first and second fixture parts may have a height of 30 mm.

[0154] This configuration allows to effectively prevent unwanted flow/displacement of the layered material from the saddle-shaped base.

[0155] Advantageously, the saddle-shaped base can be made of high-density polyethylene (HDPE).

[0156] Further details and advantages of the present invention shall now be disclosed in connection with the drawings, where:

Fig. 1 is photographic reproduction of an exemplary 3D-printed body made of a lattice structure for use in a protective pad for a cycling garment according to the invention, said lattice structure being made of a plurality of grid cells formed by crossing beams defining a void therebetween;

Fig. 2 is a front view in vertical cross-section of the protective pad according to the invention;

Fig. 3 is a front view in vertical cross-section similar to that of **Fig. 2,** but where the section plane is located at a different point of the protection pad;

Fig. 4 is a photographic reproduction of a measurement saddle for use in a method for measuring pressure distribution at the human-saddle interface on a static cycle, e.g.

a smart bike, according to an embodiment of the present invention;

Fig. 5 is a photographic reproduction of a 3D scanner setup for implementing a 3D-scanning process of a mold obtained by using the measurement saddle of **Fig. 4;**

Fig. 6 is a diagram showing the definition of the characteristic load values, obtained by using the measurement saddle of **Fig. 4** in the context of an experimental study involving 29 female serious road cyclists. Here, cx is marked by a vertical line intersecting the x axis at 140 mm, while cz is marked by a horizontal line, intersecting the y axis at approximately 27 mm;

Fig. 7 is a diagram showing data point lattices after digitizing molds, obtained by using the measurement saddle of **Fig. 4,** in the above-mentioned experimental study. The mold height is shown for a lattice with equidistant spacing of 5 mm in the x-y plane.

Here, loading was dynamic. In detail: Fig. 7a mold 8 - the anterior region is marked by low mold height alongside material deformation. The posterior region shows a spherical imprint along the longitudinal axis. Fig. 7b mold 13 - a small imprint is shown in the anterior region of the saddle, while close to no imprint can be seen in the posterior region;

Fig. 8 is a diagram showing statically loaded mold 12 in the above-mentioned experimental study, in contour lines. A height of 30 mm is labeled, presenting the initial plasticine material height. A clear shift in the loading towards the left pelvis is visible and in alignment with a left shoulder injury affecting the involved participant;

Fig. 9 is a diagram showing mean mold height along the longitudinal axis in both the static measurement (Fig. 9a) and the dynamic measurement (Fig. 9b). The shaded region is equivalent to one standard deviation. A black dashed line at the mold height of 30 mm represents the initial mold height before loading. Larger impressions, representing greater pressure, are observed with the dynamic loading as opposed to static loading;

Fig. 10 shows a CAD model of a protective pad for a cycling garment, developed in the context of the above-mentioned experimental study. The cross section shows the distribution of beam diameters according to the measured pressure distributions. The large pressure in the anterior pelvic region results in the provision of greater beam diameters, providing a higher thickness. The impression of the ischial tuberosities was hardly noticeable in the measurements carried out during the experimental study, so the pad model only shows slight variations in the lattice structure concerning this area.

[0157] **Fig. 1** shows a schematic overview of 3D-printed body made of a lattice structure, for use in a protective pad 100 for a cycling garment according to the invention.

[0158] Also, **Figs. 2-3** show different cross-section views of the protective pad 100 according to the invention.

[0159] The protective pad 100 includes a 3D-printed body 10 made of a lattice structure 12, as shown in **Fig. 1.**

[0160] In particular, said lattice structure 12 comprises different regions characterized by at least one different mechanical property.

[0161] In the present embodiment, said mechanical property includes thickness.

[0162] Therefore, the lattice structure 12 is characterized by the presence of different regions having a different thickness.

[0163] In the shown embodiment, the lattice structure 12 comprises a grid made of a plurality of grid cells 14, each including crossing beams 16 defining a void 18 therebetween **(Figs. 1-3).**

[0164] In particular, grid cells 14 defining regions of the lattice structure 12 having a higher thickness include beams 16 which are larger in cross-section **(Fig. 3).**

[0165] On the other hand, grid cells 14 defining regions of the lattice structure 12 having a reduced thickness include beams 16 which are smaller in cross-section **(Fig. 2).**

[0166] The regions of the lattice structure 12 having a higher thickness as shown, e.g., in **Fig. 3,** correspond to regions that are subject to a higher pressure load at the human-saddle interface in a riding position.

[0167] On the other hand, the regions of the lattice structure 12 having a reduced thickness as shown, e.g., in **Fig. 2,** correspond to regions that are subject to a lower pressure load at the human-saddle interface in a riding position.

[0168] Therefore, improved dampening can be provided where the pressure load is higher during riding.

[0169] For instance, said riding position can be a position on the drops.

[0170] Alternatively, said riding position can be a position on the tops.

[0171] As a further alternative, said riding position can be a position for time-trial.

[0172] The present invention further provides a cycling garment (not shown) including the protective pad 100 described above.

[0173] Said cycling garment can be one among cycling shorts, a cycling suit or a triathlon suit.

[0174] In the present embodiment, said cycling garment is specifically designed for the anatomy of a female cyclist, preferably a female road cyclist.

[0175] Also, the present invention provides a method for measuring pressure distribution at the human-saddle interface on a static cycle.

[0176] Advantageously, said static cycle can be a smart bike according to the state of the art.

[0177] The method comprises performing a cycle-fitting process when a participant is pedaling while sitting on a saddle of the static cycle in a riding position.

[0178] In the present embodiment, said cycle-fitting process comprises:

collecting anthropometric data of said participant, in particular in a standing position of said participant and/or while pedaling in the riding position of said participant, and

implementing a real-time algorithm for defining optimized parameters for adjusting at least a position, height and inclination of saddle, a position of the handlebar and crank arm lengths, based at least on the collected anthropometric data of the participant.

[0179] In particular, in the present embodiment, the cycle-fitting process is performed while the participant is pedaling on the static cycle for 15 minutes at 60 rpm and 100W, in the riding position.

[0180] In particular, in the present embodiment, said anthropometric data of the participant include one or more among:

hip width,

hip rotation angle, and/or

lumbar angle.

[0181] Preferably, said anthropometric data include a combination of hip width, hip rotation angle and lumbar angle.

[0182] In particular, the hip rotation angle is measured in the sagittal plane between the thigh and lumbar spine alignment when performing a maximum possible forward bend.

[0183] In particular, the lumbar spine angle is defined by the angle between the lumbar and thoracic spine orientation in the same forward bend.

[0184] Preferably, said anthropometric data of the participant are collected by using a depth-sensing camera.

[0185] Preferably, in the present embodiment, the definition of optimized parameters for adjusting at least a position, height and inclination of the saddle, a position of the handlebar, and crank arm lengths are further based on:

a pain status of the participant, and/or

continuously measured joint angles.

[0186] The method further includes the following steps of:

providing a measurement saddle 200 (e.g. as shown in **Fig. 4** and further described in the following);

layering a first amount of a plastically deformable material on a carrier structure 20 of the measurement saddle 200;

providing a cover on said plastically deformable material, layered on the carrier structure 20 of the measurement saddle 200;

replacing the saddle of the static cycle with the measurement saddle 200;

forming a first mold 30 in a dynamic condition, while the participant is pedaling on the measurement saddle 200 in the riding position;

removing the first mold 30 from the measurement saddle 200;

layering a new amount of plastically deformable material on the carrier structure 20 of the measurement saddle 200;

providing a cover on said plastically deformable material, layered on the carrier structure 20;

forming a second mold 40 in a static condition, while the participant is sitting on the measurement saddle 200 in the riding position with the crank arms of the static bike placed in a horizontal position,

removing the second mold 40 from the measurement saddle 200;

performing a 3D-scanning process of the first mold 30 and the second mold 40;

superimposing the obtained 3D-scans along a reference coordinate system, and

implementing software means for generating a surface model of the superimposed 3D-scans and obtaining data regarding individual load patterns at the human-saddle interface for the participant.

[0187] An exemplary setup of a 3D-scanner of the kind used in the experimental study described below is shown in **Fig. 5.**

[0188] In particular, in the present embodiment, the step of forming the first mold 30 is performed while the participant is pedaling on the static cycle for 20 minutes at 60 rpm and 100W in the riding position.

[0189] In particular, in the present embodiment, the step of forming the second mold 40 is performed while the participant is sitting on the measurement saddle 200 in the riding position for 20 minutes, changing the left/right foot position after the first 10 minutes.

[0190] For instance, said riding position can be a position on the drops, as in the experimental study described below.

[0191] Alternatively, said riding position can be a position on the tops.

[0192] As a further alternative, said riding position may be a position for time-trial.

[0193] In the present embodiment, the step of layering the plastically deformable material on the carrier structure 20 of the measurement saddle 200 comprises providing a first layer and a second layer of said plastically deformable material on said carrier structure 20.

[0194] In particular, in the present embodiment, each of said first and second layers has a height of 15 mm.

[0195] Advantageously, in the present embodiment, the method further includes providing a mark 50 (as shown, e.g., in **Fig. 5**) on both the first mold 30 and the second mold 40 at a predefined location along the longitudinal axis of the carrier structure 20, for use as reference points in 3D-scanning and data analysis.

[0196] For example, said mark 50 may be carved in the molds 30, 40 **(Fig. 5).**

[0197] The 3D-scanning process is carried out by placing each of the first and second molds 30, 40 on a rotary plate 60 after covering each of the first and second molds 30, 40 with a chalk spray.

[0198] An exemplary rotary plate 60, as used in the experimental study described below, is shown in **Fig. 5.**

[0199] In the present embodiment, the method further comprises removing (e.g., through cutting by using a knife)

residual plastically deformable material protruding from the bottom end of the first and second molds 30, 40, to ensure a planar position for the 3D-scanning process.

[0200] Also, after replacement of the saddle of the static bike with the measurement saddle 200, the method further includes dropping the seatpost of the static cycle of 15 mm. Accordingly, the reference position obtained through the cycle-fitting process can be achieved considering the height differences between the saddle of the cycle, e.g. a smart bike, and the measurement saddle 200.

[0201] The present invention further provides a method of manufacturing the protective pad 100 described above.

[0202] In particular, the method comprises:

implementing the above-described method for measuring pressure distribution at the human-saddle interface on a static cycle for at least one participant, to obtain data regarding individual load patterns at the human-saddle interface for said at least one participant;

generating a digital mold model of the lattice structure, based on said data regarding individual load patterns at the human-saddle interface so obtained for the at least one participant, and

implementing a 3D printing process for manufacturing the protective pad 100, based on the generated 3D model.

[0203] In particular, in the present embodiment, the method comprises:

implementing the above-described method for measuring pressure distribution at the human-saddle interface on a static cycle, for obtaining data regarding individual load patterns at the human-saddle interface for each participant of said plurality of participants, and

generating an average reference data set based on the obtained data regarding individual load patterns at the human-saddle interface for said plurality of participants.

[0204] In particular, the digital mold model of the lattice structure is generated based on said average reference data set.

[0205] In the present embodiment, said plurality of participants includes a plurality of female cyclists.

[0206] Preferably, said plurality of female cyclists includes a plurality of female road cyclists, as in the below-described experimental study.

[0207] The present invention further provides a measurement saddle 200 for use in the above-described method for measuring pressure distribution at the human-saddle interface on a static cycle.

[0208] An embodiment of the measurement saddle 200 according to the invention is shown in **Fig. 4.**

[0209] In particular, the measurement saddle 200 includes:

a carrier structure 20 comprising:

a saddle-shaped base 22, acting as a level surface, and

a plurality of fixture parts 24, 26, configured and adapted for acting as boundaries for a plastically deformable material, to prevent material flow, and

a saddle rail 28.

[0210] In the present embodiment, the carrier structure 20 has a length of 250 mm and a maximum width of 210 mm.

[0211] In the present embodiment, said plurality of fixture parts 24, 26 includes:

a first fixture part 24, connected to the anterior end of said saddle-shaped base 22, and

a second fixture part 26, connected to the posterior end of said saddle-shaped base 22.

[0212] Preferably, said first and second fixture parts 24, 26 have a height of 30 mm.

[0213] Preferably, the saddle-shaped base 22 is made of high-density polyethylene (HDPE).

Experimental study on 29 experienced female road cyclists

Introduction

[0214] An experimental study has been conducted by the inventors on 29 experienced female road cyclists in order to investigate the relationship between pressure distribution at the human-saddle interface and health risks in terms of pain and/or injuries and/or discomfort in the pelvic and/or genital region while riding.

[0215] The age of the participants was between 21 and 63 years (mean=32 years, SD=9.92 years).

[0216] The inclusion criteria for the participants were a minimum age of 18 years, female sex and experience in road cycling, being defined as a minimum of one cycling tour of 1.5 hours per week.

[0217] Data acquisition took place via social media and from inventor's acquaintances.

[0218] Exclusion criteria were an acute Covid-19 disease and acute pain with relevant influence on the seating position.

[0219] The characteristics (mean, SD) of the participants in terms of size, age and weight are resumed in **Table 1.**

Table 1

	Mean	SD
Size [cm]	169	5.9
Age [yrs]	32.0	9.9
Weight [kg]	62.1	7.7

[0220] The distribution of the cycling mileage per year and active years of cycling for the participants is shown in **Table 2.**

Table 2

	[km/yr]	Distribution [%]
Cycling mileage	<1000	3.4
	1000-3000	34.5
	3000-5000	27.6
	>5000	34.5
Active cycling years [yrs]	<1	10.3
	1-3	51.7
	3-5	10.3
	>5	27.6

[0221] A questionnaire collected information on the frequency of the following cycle-related complaints in terms of:

- injuries in the genital area or the area of ischial tuberosities;
- discomfort in the genital area;
- discomfort in the area of the ischial tuberosities;
- skin irritations in the genital area;
- skin irritations in the area of the ischial tuberosities,
- swellings in the genital area and numbness in the genital area.

Measurement saddle and measurement criteria

[0222] Pressure distribution measurements were taken with a measurement saddle that was specifically developed for this experimental study, and then digitized in order to process the results.

[0223] In particular, the measurement saddle corresponds to the measurement saddle 200 described above and shown in **Fig. 4.**

[0224] Soft plasticine (Super Soft, Creall, AH Ermelo, The Netherlands) showed the most appropriate deformation ranges as a plastically deformable material in the context of the present study.

[0225] It was inserted in two layers of 15 mm each between the fixture parts of the carrier structure of the measurement saddle.

[0226] The plastically deformable material was reusable in multiple measurements thanks to its ability to deform

reversibly without change to its properties.

[0227] A commercially available cling film was used to cover the plasticine in the experiments.

[0228] The measurement saddle was completed by a commercially available saddle rail and clamp to allow attachment to the existing seatposts of a smart bike.

[0229] The locally appearing pressure values were assumed to be proportional to the material displacement of the plastically deformable material.

[0230] The pressure distribution was, therefore, measured qualitatively.

[0231] This approach allowed for a higher resolution of pressure distribution on the seating surface, and ensured accurate measurements independent of the specific, underlying saddle geometry.

[0232] All collected data were saved pseudonymously and with the written approval of the participants.

[0233] For the experiments, participants wore sport tights without any type of padding and cycling shoes with cleats.

[0234] Measurements were made at room temperature.

[0235] All 29 participants completed the study.

[0236] Experimental data were collected during a session of approximatively 90 minutes for each participant, using a smart bike according to the state of the art.

[0237] Each session consisted essentially in three subsequent steps:

(i) Bike-fitting (smart bike setup);

(ii) Dynamic measuring in a riding position;

(iii) Static measuring in a riding position.

(i) Bike-fitting

[0238] A bike-fitting process was implemented for each participant by using idmatch smart bike (idmatch, Selle Italia, Casella d'Asolo, Italy).

[0239] Here, anthropometric data were collected for each participant through an integrated depth-sensing camera as part of the bike-fitting process, said anthropometric data including hip width, hip rotation angle and lumbar angle.

[0240] In particular, the hip rotation angle was measured in the sagittal plane between the thigh and lumbar spine alignment when performing the maximum possible forward bend.

[0241] The lumbar spine angle was defined by the idmatch system as the angle between the lumbar and thoracic spine orientation in the same forward bend.

[0242] The same collected data were also later used for correlation analyses.

[0243] Then, a real-time algorithm was implemented to vary the saddle and handlebar position based on the participant's anthropometry, pain status and continuously measured joint angles.

[0244] Then, the participant sat on the smart bike saddle and pedaled for about 15 minutes at 60 rpm and 100W in the drops position.

[0245] The suggested optimum position for the participant was defined by the height and horizontal position of the saddle, handlebar height and crank arm length.

[0246] To validate the positions, vertical distances between the top of the handlebar and the top of the saddle were compared to current recommendations.

[0247] The suggested position for each individual participant was defined as the reference position for the subsequent pressure distribution measurements.

(ii) Dynamic measurement in a riding position

[0248] After completion of the smart bike setup, the smart bike saddle was replaced by the measurement saddle.

[0249] Due to height differences between the smart bike saddle and the measurement saddle, the seatpost was dropped 15 mm to achieve the reference position defined during the bike-fitting process.

[0250] The participant then pedaled at 60 rpm and 100W in the drops position for 20 minutes while the mold formed.

(iii) Static measurement in a riding position

[0251] As a reference, a second, static measurement was performed by using the measurement saddle.

[0252] The mold formed during the dynamic measurement was removed from the measurement saddle and replaced with fresh soft plasticine.

[0253] Then, the participant sat in the reference position for 20 minutes with crank arms in a horizontal position.

[0254] The right and left foot positions were switched after 10 minutes.

3D scanning and generation of characteristic load values

[0255] As reference points for the subsequent 3D scan and data analysis, two marks were carved in the plasticine of each mold (dynamic and static).

[0256] In particular, said marks were located at predefined positions on the longitudinal axis of the carrier structure **(Fig. 5).**

[0257] The protruding plasticine on the bottom end of the molds was cut with a knife to ensure a planar position of the mold during the subsequent 3D-scanning process.

[0258] After removal from the measurement saddle, and once separated from the cling film, the molds were coated with commercial chalk spray (133985, Motip Dupli, Haßmersheim, Germany) and then placed on a rotary plate to be scanned with a 3D-scanner (Space Spider, Artec, Luxembourg, Luxembourg).

[0259] The 3D-scanner was placed on a standard tripod and calibrated using markers on the table. 360-degree scans were taken from three respective positions for each mold to complete the digital 3D body **(Fig. 5).**

[0260] The resulting 3D Scans were equally aligned along a reference coordinate system using CAD software (Inventor Professional, Autodesk, Munich, Germany).

[0261] The previously carved marker in the plasticine provided the position for the reference coordinate system **(Fig. 5).**

[0262] An equidistant lattice of 5 mm cell size was superimposed on the top surface of the digital mold models.

[0263] Assuming the observed discomfort rating in the questionnaire as being related to the deformation distribution along the longitudinal axis, two characteristic load values were chosen to quantify deformation behavior: cz, representing the minimum height of the mold along this axis of the saddle, and ex, defining the position of that minimum.

[0264] The definition of the characteristic load values is shown in **Fig. 6.**

[0265] In this study, the impression depths of the molds were equated to the applied loading and thus neglected the material properties and material flow.

[0266] Correlations were investigated in the static and dynamic results independently.

[0267] Using Shapiro-Wilk tests ($\alpha = 0.05$), the distribution of the non-ordinal data, namely hip width, lumbar angle, hip rotation angle, cx and cz, were determined to choose an appropriate statistical method. Spearman's rank-order was used to correlate the characteristic load values cx and cz independently with each complaint of the athletes stated in the questionnaire or gained from the bike-fitting process.

[0268] Given a normal distribution of the metric data, Pearson's correlation was additionally used to evaluate potential relations.

Definition of a protective pad design

[0269] The generated data point lattices of the digital molds, which had proven to be representative of pressure distribution, were used to define the design of an innovative protective pad for use in a cycling garment, such as cycling shorts, specifically designed for women.

[0270] The 29 generated data point clouds of the dynamic experiment were combined into one average reference data set.

[0271] A cubic unit cell with an edge length of 5 mm, body-centered diagonal beams and face-centered horizontal beams served as a basis for the lattice.

[0272] It was used to fill the pad geometry, which was a 7.5 mm high, extruded profile with the shape of a cycling garment pad, e.g. a cycling short pad.

[0273] According to local pressure values, beam diameters of the respective unit cells were adapted, which led to a heterogeneous lattice structure within the protective pad.

[0274] CAD models of protective pads were designed using CAD software (Creo ProEngineer, PTC, Unterschleissheim, Germany).

Results

[0275] The questionnaire results revealed discomfort in the genital and/or pelvic area to be the most common complaint with 37.9% of the participants suffering from it "often" or "always".

[0276] The posterior region of the ischial tuberosities was found to be less affected, with only 10.3% of the participants stating that they experienced discomfort "often" or "always".

[0277] The majority of the participants (65.5%) stated that they suffer from skin irritation in the genital area at least "sometimes", making it the second leading complaint in the context of the present study.

[0278] All shares of participants suffering from complaints related to serious road cycling are listed in **Table 3.**

Table 3

Due to road cycling, I experience...	Never	Rarely	Sometimes	Often
... injuries in the genital or pelvic area	51.72	17.24	24.14	3.45
...discomfort in the genital or pelvic area	10.34	13.79	37.93	34.48
... discomfort in the area of the ischial tuberosities	20.69	48.28	20.69	10.34
... skin irritations in the genital area	17.24	17.24	34.48	27.59
... skin irritations in the area of the ischial tuberosities	58.62	34.48	6.90	0.00
... swelling in the genital area	31.03	34.48	27.59	6.90
... numbness in the genital area	48.28	31.03	13.79	6.90

[0279] Shapiro-Wilk tests showed evidence of a potential normality for the following data: lumbar angle (p = 0.75) and cz (p = 0.31), both in the static experiment.

[0280] A Pearson correlation showed no significance for the data pairs.

[0281] Calculating the Spearman's rank coefficient, a significant correlation is found in two cases for the static data.

[0282] Between the hip rotation angle and cz (p = -0.38, p = 0.05), a weak to moderate correlation existed (R^2 = 0.14).

[0283] Numbness in the genital area and cz showed a moderate correlation (ρ = -0.47, p = 0.01) with R^2 = 0.22.

[0284] Considering the overall quality of the molds, the developed measurement device was found to deliver detailed data.

[0285] Clear individual loading patterns could be observed in the molds.

[0286] The data point lattice of two different molds in the dynamic experiment are shown in **Fig 7.** In particular, Fig. 7a refers to mold 8, while Fig. 7b refers to mold 13.

[0287] The anterior region of mold 8 shows large material deformation accompanied by a large impression depth (Fig. 7a).

[0288] In the posterior region, a spherical imprint can be seen along the longitudinal axis.

[0289] In comparison, mold 13 (Fig. 7b) shows a much lower deformation of the anterior region and no visible deformation in the posterior region.

[0290] Individual injuries are reflected in the measurements.

[0291] As an example, **Fig. 8** shows a representation of statically-loaded mold 12 in contour lines, referring to a participant affected by an injury in the left shoulder. A height of 30 mm was labeled, presenting the initial plasticine material height. A clear shift in the loading towards the left pelvis is visible and in alignment with the left shoulder injury of the participant.

[0292] In particular, the left shoulder injury of the participant resulted in a higher loading of the left pelvis region in both the static and dynamic experimental measurements.

[0293] Besides being relevant for the correlation analyses, the defined characteristic load values allowed for a quantitative analysis of the measured pressure distribution.

[0294] In the static experiment, cx varied between 110 mm and 215 mm (mean=151.07, SD=23.90) with 215 mm representing the most anterior, and 110 mm the most posterior seating position in the study.

[0295] One mold of the static study showed a cx value of 0 and was, therefore, excluded from further processing. *cz* varied between 30.5 mm and 21.3 mm (mean=25.97, SD=2.78).

[0296] For the dynamic loading situation, the molds showed a cx value between 105 mm and 170 mm (mean=150.52, SD=16.50).

[0297] For cz, the minimum value was 15.5 mm and the maximum value was 29.8 mm (mean=24.33, SD=3.72).

[0298] **Fig. 9** shows the mean mold height for both static (Fig. 9a) and dynamic (Fig. 9b) measurements in cross section along the longitudinal axis.

[0299] Here, the shaded region is equivalent of one standard deviation.

[0300] The black dashed line at mold height of 30 mm represents the initial mold height before loading.

[0301] The mean and standard deviations were calculated for each value on the x-axis and displayed in the plot as the line and the shaded region, respectively.

[0302] In particular, as shown in **Fig. 9,** the standard deviation of the dynamic measurements is larger along the entire longitudinal axis than the one of the static measurements.

[0303] The above findings had proven that the used measurement saddle delivered valuable data, which can be used to develop an improved protective pad for a cycling garment, e.g. cycling shorts, in particular designed for female road cyclists.

[0304] **Fig. 10** shows a CAD model of a prototype of the developed protective pad, in cross-section.

[0305] The lattice parameters, namely the beam diameters, vary within the pad according to the measured pressure distribution.

[0306] Larger beam diameters of up to 2.8 mm were created in the anterior pelvic area, while the posterior area of the pad consisted mainly of smaller beam diameters up to a minimum of 1.5 mm. Also, at the borders of the widening posterior part, larger beam diameters were created due to more intense thigh contact.

Discussion

[0307] The proportions of participant athletes reporting genital pain, discomfort and numbness in the present study are in line with the studies of Larsen et al., Hermans et al. and Guess et al. **[3], [4], [7].**

[0308] In the present study, the relationship between the characteristic load values and the most common complaints, as well as the anthropometric data, were investigated.

[0309] Interestingly, the results showed correlations only for the static measurements.

[0310] This could indicate, that cycling duration might not play a crucial role in measuring pressure distribution.

[0311] A moderate correlation was found between genital numbness and the maximum impression depth cz, yet it is deemed that this correlation should be treated with caution.

[0312] The coefficient of determination (R^2) suggests that only about 22% of the variability of genital numbness can be explained by the relationship with the amount of anterior loading.

[0313] This means that 78% must be due to at least one other factor related to genital numbness.

[0314] With respect to anthropometric data, a weak to moderate correlation was found between the hip rotation angle and *cz*.

[0315] R^2 shows, that only 14% of the variability of hip flexibility in terms of small hip rotation angles could be related to large anterior loading.

[0316] The hip rotation angle data shows signs of clustering because the measured angles are limited to 51, 59, 68 and 78 degrees.

[0317] This might be an indicator for insufficient data quality.

[0318] Further, it should be considered that another possible cause for the lack of strong correlations might be the relatively small number of participants or the subjective assessment of, for example, discomfort.

[0319] This is underlined by an earlier study, in which cycling athletes stated both to be comfortable and suffer from pain simultaneously **[24].**

[0320] The present study was carried out with individual reference positions based on the above-mentioned idmatch bike-fitting.

[0321] Indeed, this excluded personal bicycle setups and might have led to different pressure distributions than the ones on a personal bicycle, which are actually underlying for the stated complaints.

[0322] Interestingly, 39% of the participants stated that bike-fitting improved their personal comfort.

[0323] A bike-fitting, as done in the present study, might, therefore, completely change the bicycle setup of the athlete and result in a different pressure distribution on the saddle.

[0324] This shows that the inclusion of personal setup pressure in further studies could represent an interesting development.

[0325] However, due to the quality of data and the inconclusive results of the correlation data, it is presently not possible to conclude that hip rotation angles are a predictor for great anterior saddle loading, or that genital numbness is related to great anterior saddle loading.

[0326] Further, the present results did not show clear signs of a relation between the pressure distribution and the complaints of the athletes.

[0327] Existing cycling garment pads for female athletes often rely on insufficient objective data **[3], [28].** The present study provides an improved design for a protective pad, which is specifically based on pressure distribution data.

[0328] In particular, by using the developed measurement saddle **(Fig. 4),** individual pressure distribution could be investigated for each of the 29 female road cyclist that took part in the experimental study in a very detailed manner **(Fig. 7).**

[0329] In particular, compared to known digital pressure distribution measurement methods, the present approach allowed to achieve a higher resolution and a representation of individual complaints **(Fig. 8).**

[0330] Pad stiffness in the anterior region is increased due to the large loads measured there. This means that, in use, the lattice deformation stays small enough to provide residual flexibility and prevent the genital area from being pushed strongly against the saddle nose.

[0331] This correlates with Larsen et al. **[3],** revealing that an unpadded contact in the crotch area led to pain after 12 weeks of use (10.3% of participants). In the control group with a padded area instead, 5.2% of athletes stated that they experienced pain.

[0332] In contrast, too soft cushioning can result in one third more loss of oxygenation, as found by Sommer et al. (unpublished data, reference is made to **[9]**). Here, the authors explained this aspect by soft matter being pressed into the

perineal region more than in unpadded seats.

[0333] The reason why the protective pad according to the present study is stiffer in the anterior region lies in the obtained results, revealing a load concentration in the anterior area and less significant loads in the posterior area.

[0334] Potter et al. and Bressel et al. observed similar distributions of pressure, but with slightly more dominant posterior pressure centers **[11], [13].**

[0335] It is probable that the greater width of the used measurement saddle in the posterior area prevented the plastically deformable material from flowing, thereby limiting deformation.

[0336] In previous versions of the measurement saddle with a smaller posterior area, a bulging of the material beyond the edges of the carrier structure was observed, which may have influenced the comparability of measurements.

[0337] By contrast, use of a softer material may cause athletes to displace too much material in the anterior area.

[0338] However, improvements are likely possible through the use of different setups.

[0339] Additionally, the present study was limited to observing pressure values in the drops position due to properties of the bike-fitting system.

[0340] Indeed, as the upper body inclines, the pressure center is found to move towards the anterior region of the saddle **[11], [15],** which may explain the small posterior pressure in the current results of the experimental study.

[0341] The comparability to the literature is limited due to the fact that the used experimental setup is not influenced by a specific underlying saddle geometry, but consists of a leveled carrier structure.

[0342] However, further studies including, e.g., a position on the tops may reveal a larger pressure at the ischial tuberosities and, therefore, result in a different distribution of stiffness in the lattice structure.

[0343] Despite the fact that every participant of the present study was fitted to her respective optimal bike position, both the maximum impression depth cz and the location of maximum load cx varied significantly (see **Fig. 9**).

[0344] These results likely underline the individual pressure distributions on the saddle despite the standardized position on the bicycle.

[0345] However, they could also beg the question of whether the bike-fitting process is suitable for providing a reference bike position for the athletes.

[0346] So far, no studies have been found that validate the algorithms used by the idmatch system.

[0347] However, the vertical distance between the top of the saddle and the top of the handlebar was 5.9 mm on average, which is in line with the recommendations of Silberman et al. **[29].**

[0348] The practical relevance of the idmatch system was also considered to not be negligible, since recommended positions are based on numerous iterative bike-fittings and athlete experiences, while being processed in a machine learning algorithm.

[0349] Given the various pressure distributions measured in the present study, it is considered that an individualized protective pad for use in a cycling garment would be beneficial for cyclists.

[0350] In further studies, high-quality results are to be expected and differences in pressure distribution will presumably only lead to small changes in the overall protective pad concept.

[0351] One aim is to be able to transfer specific pressure distributions to a customized pad design using the developed approach.

Bibliography

[0352]

[1] Oja P, Titze S, Bauman A et al. Health benefits of cycling: a systematic review. Scand J Med Sci Sports 2011. 21: 496-509.

[2] Gaither TW, Awad MA, Murphy GP et al. Cycling and female sexual and urinary function: Results from a large, multinational, cross-sectional study. J Sex Med 2018. 15: 510-518.

[3] Larsen AST, Norheim KL, Marandi RZ et al. A field study investigating sensory manifestations in recreational female cyclists using a novel female-specific cycling pad. Ergonomics 2021. 64: 571-581.

[4] Hermans TJN, Wijn R, Winkens B et al. Urogenital and sexual complaints in female club cyclists - a cross-sectional study. J Sex Med 2016. 13: 40-45.

[5] Greenberg DR, Khandwala YS, Breyer BN et al. Genital pain and numbness and female sexual dysfunction in adult bicyclists. J Sex Med 2019. 16: 1381-1389.

[6] Lui HS, Mmonu N, Awad MA et al. Association of bicycle-related genital numbness and female sexual dysfunction: Results from a large, multinational, cross-sectional study. J Sex Med 2021. 9.

[7] Guess MK, Connell K, Schrader S et al. Genital sensation and sexual function in women bicyclists and runners: are your feet safer than your seat? J Sex Med 2006. 3: 1018-1027.

[8] Taylor KS, Richburg A, Wallis D et al. Using an experimental bicycle seat to reduce perineal numbness. Phys Sportsmed 2002. 30: 27-+.

[9] Sommer F, Goldstein I and Korda JB. Bicycle riding and erectile dysfunction: A review. J Sex Med 2010. 7: 2346-2358.
[10] Partin SN, Connell K, Schrader S et al. Les lanternes rouges: The race for information about cycling-related female sexual dysfunction. J Sex Med 2014. 11: 2039-2047.
[11] Potter JJ, Sauer JL, Weisshaar CL et al. Gender differences in bicycle saddle pressure distribution during seated cycling. Med Sci Sports Exerc 2008. 40: 1126-1134.
[12] Guess MK, Partin SN, Schrader S et al. Women's bike seats: a pressing matter for competitive female cyclists. J Sex Med 2011. 8: 3144-53.
[13] Bressel E, Bliss S and Cronin J. A field-based approach for examining bicycle seat design effects on seat pressure and perceived stability. Appl Ergon 2009. 40: 472-476.
[14] Hoffmann S. The Experimental Investigation of Pressure Distribution of the Body Weight on a Road Bike Ergometer with Different Cycling-Pads. Master Thesis, Technical University of Munich, Munich 2019.
[15] Sauer J, Potter J, Weisshaar C et al. Influence of gender, power, and hand position on pelvic motion during seated cycling. Med Sci Sports Exerc 2008. 39: 2204-11.
[16] Carpes FP, Dagnese F, Kleinpaul JF et al. Bicycle saddle pressure: Effects of trunk position and saddle design on healthy subjects. Urol Int 2009. 82: 8-11.
[17] Braun-Falco O, Plewig G and Wolff HH. Erkrankungen des äußeren weiblichen Genitales. Berlin, Heidelberg: Springer Berlin Heidelberg 1984. pp. 731-736.
[18] Leibovitch I and Mor Y. The vicious cycling: Bicycling related urogenital disorders. Eur Urol 2005. 47: 277-287.
[19] Jeong SJ, Park K, Moon JD et al. Bicycle saddle shape affects penile blood flow. Int J Impot Res 2002. 14: 513-517.
[20] Lowe BD, Schrader SM and Breitenstein MJ. Effect of bicycle saddle designs on the pressure to the perineum of the bicyclist. Med Sci Sports Exerc 2004. 36: 1055-1062.
[21] Larsen AS, Larsen FG, Sorensen FF et al. The effect of saddle nose width and cutout on saddle pressure distribution and perceived discomfort in women during ergometer cycling. Appl Ergon 2018. 70: 175-181.
[22] Keytel LR and Noakes TD. Effects of a novel bicycle saddle on symptoms and comfort in cyclists. SAMJ S Afr Med J 2002. 92: 295-298.
[23] Bury K, Leavy JE, Lan C et al. A saddle sores among female competitive cyclists: A systematic scoping review. J Sci Med Sport 2021. 24: 357-367.
[24] Bini RR and Hunter JR. Pain and body position on the bicycle in competitive and recreational road cyclists: A retrospective study. Sports Biomech 2021: 1-14.
[25] De Bruyne G, Aerts JM and Berckmans D. Efficiency of Cycling Pads in Reducing Seat Pressure During Cycling, vol. 777 of Advances in Intelligent Systems and Computing. Cham: Springer International Publishing Ag 2019. pp. 38-47.
[26] Marcolin G, Panizzolo FA, Paoli A et al. Experimental methods for the mechanical characterization of cycling short pads. Proc Inst Mech Eng P J Sport Eng Technol 2018. 232: 22-27.
[27] Raccuglia M, Sales B, Heyde C et al. Clothing comfort during physical exercise-determining the critical factors. Appl Ergon 2018. 73: 33-41.
[28] Mellion MB. Common cycling injuries - management and prevention. Sports Med 1991. 11: 52-70.
[29] Silberman MR, Webner D, Collina S et al. Road bicycle fit. Clin J Sport Med 2005. 15: 271-276.

References

[0353]

100 Protective pad (for cycling garment)

10 3D-printed body
12 Lattice structure (3D-printed body)
14 Grid cells (of the lattice structure)
16 Beams (of the grid cells)
18 Voids (of the grid cells)

200 Measurement saddle

20 Carrier structure
22 Saddle-shaped base
24 First fixture part

26 Second fixture part
28 Saddle rail

30 First mold (dynamic measurement)
40 Second mold (static measurement)
50 Mark (provided on the first and second molds, respectively)
60 Rotary plate

Claims

1. A protective pad (100) for a cycling garment, said pad (100) including a 3D-printed body (10) made of a lattice structure (12), wherein said lattice structure (12) comprises different regions **characterized by** at least one different mechanical property.

2. The protective pad (100) according to claim 1,
characterized in that
said at least one mechanical property includes thickness.

3. The protective pad (100) according to claim 1 or 2,
characterized in that
the lattice structure (12) is a grid made of a plurality of grid cells (14) each including crossing beams (16) defining a void (18) therebetween.

4. The protective pad (100) according to claim 3,
characterized in that

grid cells (14) defining regions of the lattice structure (12) having a higher thickness include beams (16) which are larger in cross-section, and
grid cells (14) defining regions of the lattice structure (12) having a reduced thickness include beams (16) which are smaller in cross-section,
preferably wherein
the regions of the lattice structure (12) having a higher thickness correspond to regions that are subject to a higher pressure load at the human-saddle interface in a riding position, and
the regions of the lattice structure (12) having a reduced thickness correspond to regions that are subject to a lower pressure load at the human-saddle interface in a riding position.

5. A cycling garment including the protective pad (100) according to any one of claims 1 to 4,

preferably wherein said cycling garment is one among cycling shorts, a cycling suit or a triathlon suit,
preferably wherein said cycling garment is specifically designed for the anatomy of a female cyclist, more preferably a female road cyclist.

6. A method for measuring pressure distribution at the human-saddle interface on a static cycle, comprising:

performing a cycle-fitting process while a participant is pedaling sitting on a saddle of the static cycle in a riding position, for adjusting at least a position, height and inclination of the saddle, a position of the handlebar and crank arm lengths;;
providing a measurement saddle (200);
layering a first amount of a plastically deformable material on a carrier structure (20) of the measurement saddle (200);
providing a cover on said plastically deformable material, layered on the carrier structure (20) of the measurement saddle (200);
replacing the saddle of the static cycle with the measurement saddle (200);
forming a first mold (30) in a dynamic condition, while the participant is pedaling on the measurement saddle (200) in the riding position;
removing the first mold (30) from the measurement saddle (200);
layering a new amount of plastically deformable material on the carrier structure (20) of the measurement saddle (200);

providing a cover on said plastically deformable material, layered on the carrier structure (20);
forming a second mold (40) in a static condition, while the participant is sitting on the measurement saddle (200) in the riding position with the crank arms of the static bike placed in a horizontal position,
removing the second mold (40) from the measurement saddle (200);
performing a 3D-scanning process of the first mold (30) and the second mold (40);
superimposing the obtained 3D-scans along a reference coordinate system, and
implementing software means for generating a surface model of the superimposed 3D-scans and obtaining data regarding individual load patterns at the human-saddle interface for the participant.

7. The method according to claim 6,
characterized in that
the cycle-fitting process comprises:

collecting anthropometric data of said participant, in particular in a standing position of said participant and/or while pedaling in the riding position of said participant, and
implementing a real-time algorithm for defining optimized parameters for adjusting at least the position, height and inclination of the saddle, the position of the handlebar and
crank arm lengths, based at least on the collected anthropometric data of the participant,
preferably wherein said anthropometric data of the participant include one or more among:

hip width,
hip rotation angle, and/or
lumbar angle,

preferably wherein:

the hip rotation angle is measured in the sagittal plane between the thigh and lumbar spine alignment when performing a maximum possible forward bend, and
the lumbar spine angle is defined by the angle between the lumbar and thoracic spine orientation in the same forward bend,
preferably wherein said anthropometric data of the participant are collected by using a depth-sensing camera.

8. The method according to claim 6 or 7,
characterized in that

the cycle-fitting process is performed while the participant is pedaling on the static cycle for 15 minutes at 60 rpm and 100 W in the riding position, and/or
the step of forming the first mold (30) is performed while the participant is pedaling on the static cycle for 20 minutes at 60 rpm and 100 W in the riding position, and/or
the step of forming the second mold (40) is performed while the participant is sitting on the measurement saddle (200) in the riding position for 20 minutes, changing the left/right foot position after the first 10 minutes,
preferably wherein said riding position is a position on the drops.

9. The method according to any one of claims 6 to 8,
characterized in that
the definition of optimized parameters for adjusting the position of the saddle, the position of the handlebar, and the crank arm lengths are further based on:

a pain status of the participant, and/or
continuously measured joint angles.

10. The method according to any one of claims 6 to 9,
characterized in that

layering the plastically deformable material on the carrier structure (20) of the measurement saddle (200) comprises providing a first layer and a second layer of said plastically deformable material on said carrier structure (20),

preferably wherein each of said first and second layers has a height of 15 mm,
preferably wherein the method further includes providing a mark (50) on both the first mold (30) and the second mold (40) at a predefined location along the longitudinal axis of the carrier structure (20), for use as reference points in 3D-scanning and data analysis,
preferably wherein the 3D-scanning process is carried out by placing each of the first and second molds (30, 40) on a rotary plate (60) after covering each of the first and second molds (30, 40) with a chalk spray.

11. A method of manufacturing the protective pad (100) for a cycling garment according to claims 1 to 4, the method comprising:

implementing the method according to any one of claims 6 to 10 for at least one participant to obtain data regarding individual load patterns at the human-saddle interface for said at least one participant;
generating a digital mold model of the lattice structure, based on said data regarding individual load patterns at the human-saddle interface so obtained for the at least one participant, and
implementing a 3D printing process for manufacturing the protective pad (100), based on the generated 3D model.

12. The method according to claim 11,
characterized in that

the method includes implementing the method according to any one of claims 6 to 10 for a plurality of participants, for obtaining data regarding individual load patterns at the human-saddle interface for each participant of said plurality of participants, and
generating an average reference data set based on the obtained data regarding individual load patterns at the human-saddle interface for said plurality of participants,
wherein the digital mold model of the lattice structure is generated based on said average reference data set, preferably wherein said plurality of participants includes a plurality of female cyclists, preferably a plurality of female road cyclists.

13. A measurement saddle (200) for use in the method according to any one of claims 6 to 10, comprising:

a carrier structure (20) comprising:

a saddle-shaped base (22), acting as a level surface, and
a plurality of fixture parts (24, 26), configured and adapted for acting as boundaries for a plastically deformable material, to prevent material flow, and

a saddle rail (28).

14. The measurement saddle (200) according to claim 13,
characterized in that

the carrier structure (20) has a length of 250 mm and a maximum width of 210 mm, and/or
said plurality of fixture parts (24, 26) includes:

a first fixture part (24), connected to the anterior end of said saddle-shaped base (22), and
a second fixture part (26), connected to the posterior end of said saddle-shaped base (22),

preferably wherein said first and second fixture parts (24, 26) have a height of 30 mm.

15. The measurement saddle (200) according to claim 13 or 14,
characterized in that
the saddle-shaped base (22) is made of high-density polyethylene (HDPE).

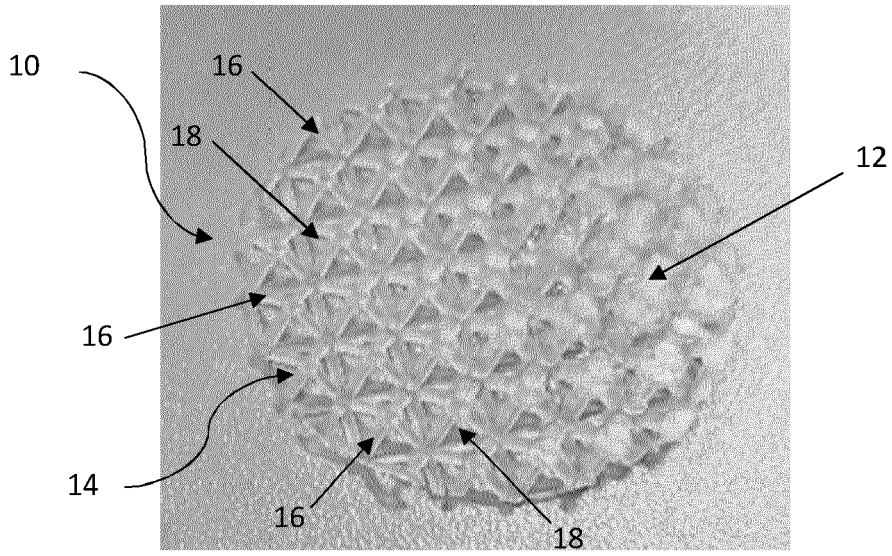

Fig. 1

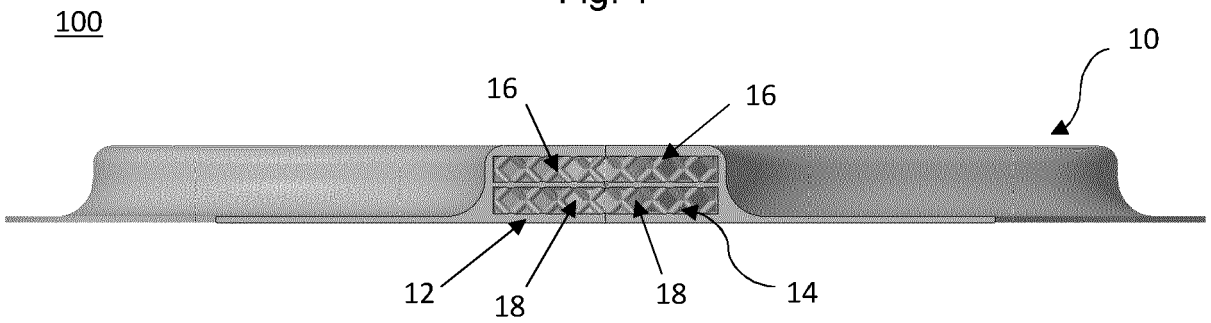

Fig. 2

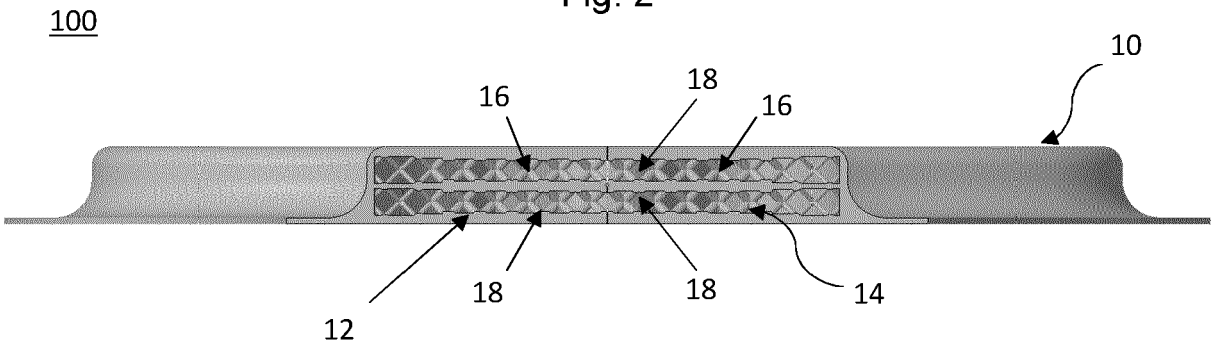

Fig. 3

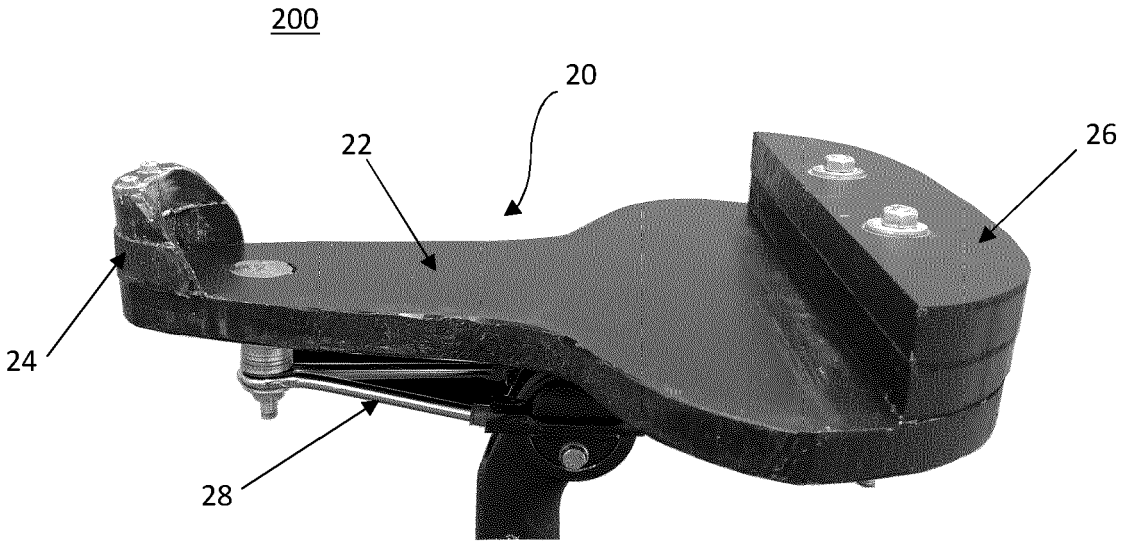

Fig. 4

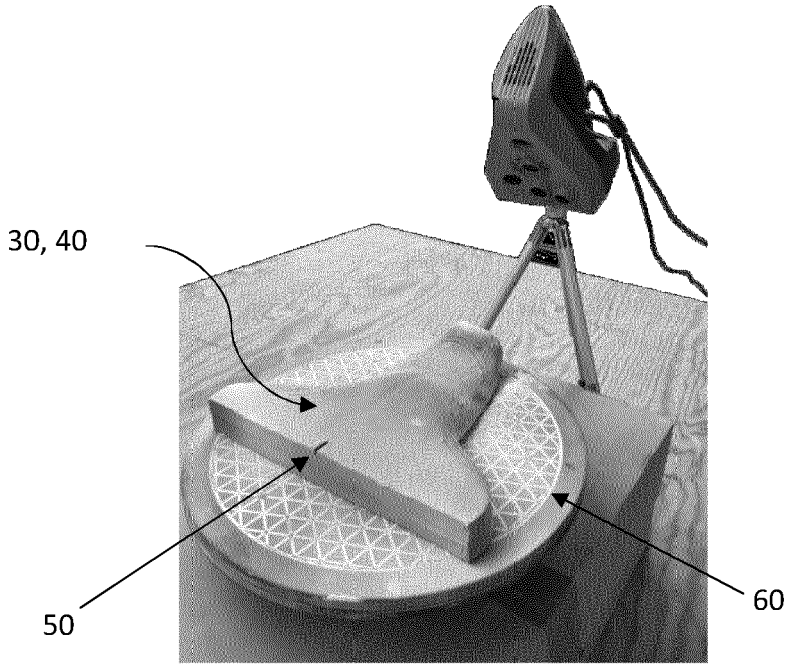

Fig. 5

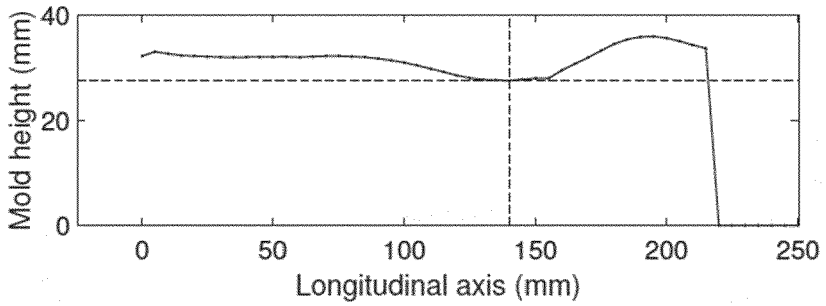

Fig. 6

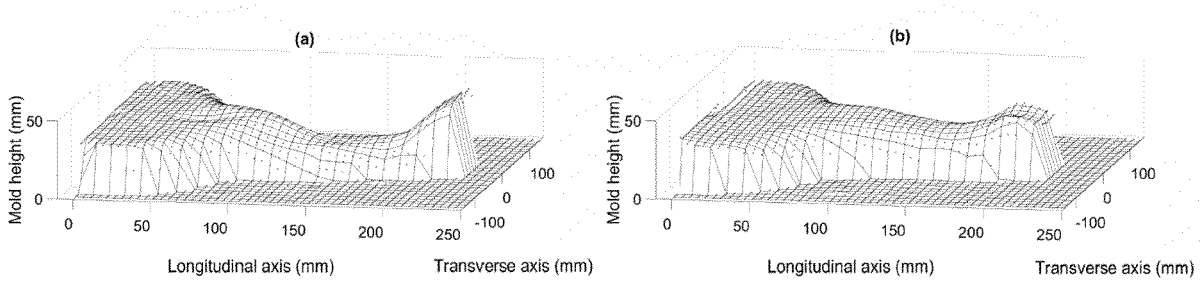

Mold 8 Mold 13

Fig. 7

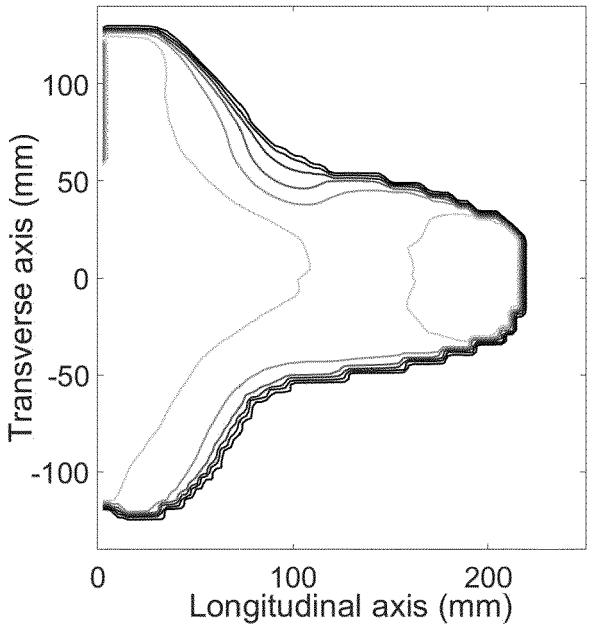

Mold 12

Fig. 8

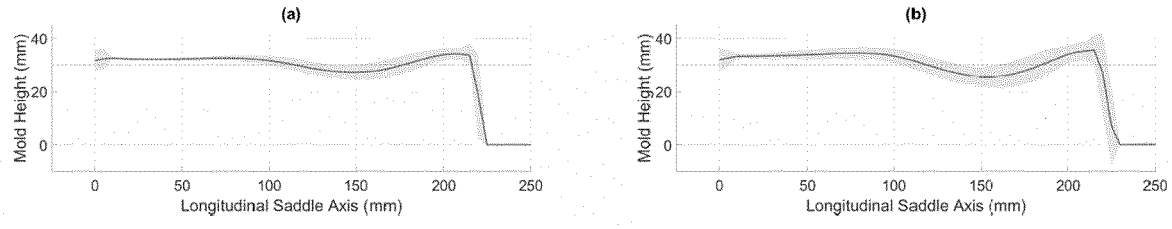

Static measurement

Dynamic measurement

Fig. 9

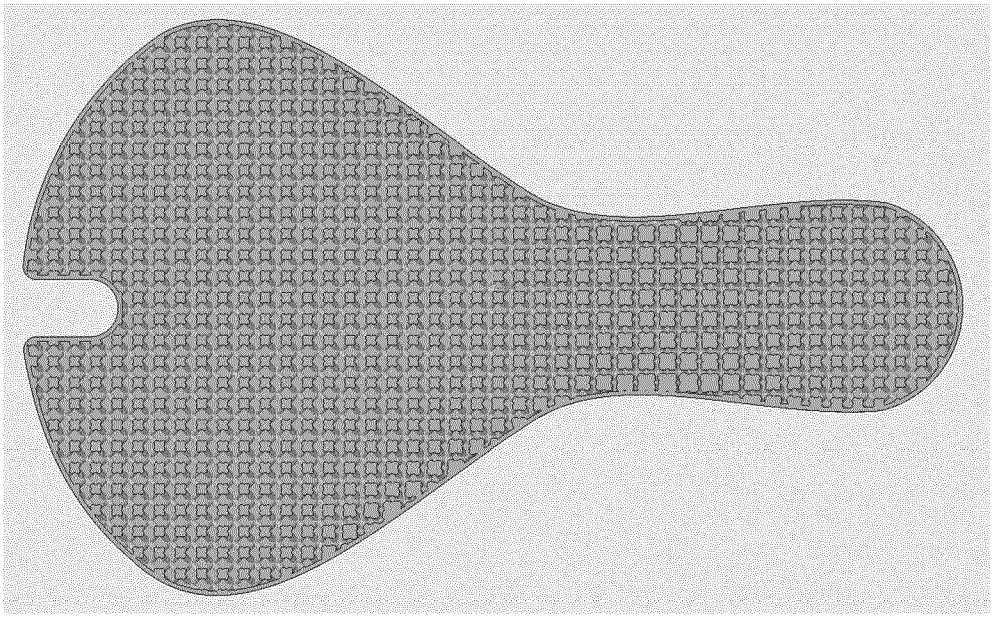

Fig. 10

Europäisches Patentamt
European Patent Office
Office européen des brevets

EUROPEAN SEARCH REPORT

Application Number
EP 23 19 0882

DOCUMENTS CONSIDERED TO BE RELEVANT

Category	Citation of document with indication, where appropriate, of relevant passages	Relevant to claim	CLASSIFICATION OF THE APPLICATION (IPC)
X	WO 2019/207444 A1 (CYTECH S R L [IT]; CANNON & MACINTOSH INVESTMENT LTD [MT]) 31 October 2019 (2019-10-31)	1-3,5	INV. A41D1/084 A41H1/02
A	* page 1, line 2 - line 4; figures 3,10 * * page 8, line 8 - line 11 *	4	
X	IT 2019 0001 6949 A1 (ENG TEAM [IT]) 30 March 2021 (2021-03-30)	1-3,5	
A	* page 1, line 1 - line 3; figure 1 *	4	
X	WO 2014/111433 A1 (KTJ KUNSTSTOFFTECHNIK JUNKER GMBH [DE]) 24 July 2014 (2014-07-24)	1-3,5	
A	* page 7, line 1 - line 3; figure 1 *	4	
X	WO 2023/053156 A1 (CYTECH S R L [IT]) 6 April 2023 (2023-04-06)	1-3,5	
A	* figures 1,6,8 *	4	
A	US 2021/294936 A1 (BARYUDIN ALAN [US]) 23 September 2021 (2021-09-23) * paragraph [0033] *	1-5	TECHNICAL FIELDS SEARCHED (IPC) A41D A41H
X	WO 2020/090798 A1 (YOSHIHARA HIROSHI [JP]) 7 May 2020 (2020-05-07)	13-15	
A	* figure 1 *	6-12	

The present search report has been drawn up for all claims

Place of search	Date of completion of the search	Examiner
The Hague	13 February 2024	van Voorst, Frank

CATEGORY OF CITED DOCUMENTS

X : particularly relevant if taken alone
Y : particularly relevant if combined with another document of the same category
A : technological background
O : non-written disclosure
P : intermediate document

T : theory or principle underlying the invention
E : earlier patent document, but published on, or after the filing date
D : document cited in the application
L : document cited for other reasons

& : member of the same patent family, corresponding document

EPO FORM 1503 03.82 (P04C01)

Europäisches Patentamt
European Patent Office
Office européen des brevets

Application Number
EP 23 19 0882

CLAIMS INCURRING FEES

The present European patent application comprised at the time of filing claims for which payment was due.

☐ Only part of the claims have been paid within the prescribed time limit. The present European search report has been drawn up for those claims for which no payment was due and for those claims for which claims fees have been paid, namely claim(s):

☐ No claims fees have been paid within the prescribed time limit. The present European search report has been drawn up for those claims for which no payment was due.

LACK OF UNITY OF INVENTION

The Search Division considers that the present European patent application does not comply with the requirements of unity of invention and relates to several inventions or groups of inventions, namely:

see sheet B

☒ All further search fees have been paid within the fixed time limit. The present European search report has been drawn up for all claims.

☐ As all searchable claims could be searched without effort justifying an additional fee, the Search Division did not invite payment of any additional fee.

☐ Only part of the further search fees have been paid within the fixed time limit. The present European search report has been drawn up for those parts of the European patent application which relate to the inventions in respect of which search fees have been paid, namely claims:

☐ None of the further search fees have been paid within the fixed time limit. The present European search report has been drawn up for those parts of the European patent application which relate to the invention first mentioned in the claims, namely claims:

☐ The present supplementary European search report has been drawn up for those parts of the European patent application which relate to the invention first mentioned in the claims (Rule 164 (1) EPC).

Europäisches Patentamt
European Patent Office
Office européen des brevets

LACK OF UNITY OF INVENTION
SHEET B

Application Number
EP 23 19 0882

The Search Division considers that the present European patent application does not comply with the requirements of unity of invention and relates to several inventions or groups of inventions, namely:

1. claims: 1-5

A protective pad for a cycling garment, a cycling garment comprising said protective pad.

---

2. claims: 6-15

A method for measuring pressure distribution at the human saddle interface on a static cycle, a method of manufacturing a protective pad implementing said measuring method and a measurement saddle for use in said method.

ANNEX TO THE EUROPEAN SEARCH REPORT ON EUROPEAN PATENT APPLICATION NO. EP 23 19 0882

This annex lists the patent family members relating to the patent documents cited in the above-mentioned European search report. The members are as contained in the European Patent Office EDP file on
The European Patent Office is in no way liable for these particulars which are merely given for the purpose of information.

13-02-2024

Patent document cited in search report	Publication date	Patent family member(s)	Publication date
WO 2019207444 A1	31-10-2019	CA 3097670 A1	31-10-2019
		CN 112236049 A	15-01-2021
		EP 3784081 A1	03-03-2021
		ES 2924378 T3	06-10-2022
		HR P20220974 T1	11-11-2022
		US 2021068475 A1	11-03-2021
		WO 2019207444 A1	31-10-2019
IT 201900016949 A1	30-03-2021	---	
WO 2014111433 A1	24-07-2014	DE 202013100221 U1	25-01-2013
		EP 2945501 A1	25-11-2015
		WO 2014111433 A1	24-07-2014
WO 2023053156 A1	06-04-2023	NONE	
US 2021294936 A1	23-09-2021	EP 3882115 A1	22-09-2021
		US 2021294936 A1	23-09-2021
WO 2020090798 A1	07-05-2020	JP 6612950 B1	27-11-2019
		JP 2020069823 A	07-05-2020
		TW 202023872 A	01-07-2020
		WO 2020090798 A1	07-05-2020

EPO FORM P0459

For more details about this annex : see Official Journal of the European Patent Office, No. 12/82

REFERENCES CITED IN THE DESCRIPTION

This list of references cited by the applicant is for the reader's convenience only. It does not form part of the European patent document. Even though great care has been taken in compiling the references, errors or omissions cannot be excluded and the EPO disclaims all liability in this regard.

Non-patent literature cited in the description

- **OJA P** ; **TITZE S** ; **BAUMAN A et al.** Health benefits of cycling: a systematic review. *Scand J Med Sci Sports*, 2011, vol. 21, 496-509 **[0352]**
- **GAITHER TW** ; **AWAD MA** ; **MURPHY GP et al.** Cycling and female sexual and urinary function: Results from a large, multinational, cross-sectional study. *J Sex Med*, 2018, vol. 15, 510-518 **[0352]**
- **LARSEN AST** ; **NORHEIM KL** ; **MARANDI RZ et al.** A field study investigating sensory manifestations in recreational female cyclists using a novel female-specific cycling pad. *Ergonomics*, 2021, vol. 64, 571-581 **[0352]**
- **HERMANS TJN** ; **WIJN R** ; **WINKENS B et al.** Urogenital and sexual complaints in female club cyclists - a cross-sectional study. *J Sex Med*, 2016, vol. 13, 40-45 **[0352]**
- **GREENBERG DR** ; **KHANDWALA YS** ; **BREYER BN et al.** Genital pain and numbness and female sexual dysfunction in adult bicyclists. *J Sex Med*, 2019, vol. 16, 1381-1389 **[0352]**
- **LUI HS** ; **MMONU N** ; **AWAD MA et al.** Association of bicycle-related genital numbness and female sexual dysfunction: Results from a large, multinational, cross-sectional study. *J Sex Med*, 2021, 9 **[0352]**
- **GUESS MK** ; **CONNELL K** ; **SCHRADER S et al.** Genital sensation and sexual function in women bicyclists and runners: are your feet safer than your seat?. *J Sex Med 2006.*, vol. 3, 1018-1027 **[0352]**
- **TAYLOR KS** ; **RICHBURG A** ; **WALLIS D et al.** Using an experimental bicycle seat to reduce perineal numbness. *Phys Sportsmed*, 2002, vol. 30, 27 **[0352]**
- **SOMMER F** ; **GOLDSTEIN I** ; **KORDA JB**. Bicycle riding and erectile dysfunction: A review. *J Sex Med 2010.*, vol. 7, 2346-2358 **[0352]**
- **PARTIN SN** ; **CONNELL K** ; **SCHRADER S et al.** Les lanternes rouges: The race for information about cycling-related female sexual dysfunction. *J Sex Med*, 2014, vol. 11, 2039-2047 **[0352]**
- **POTTER JJ** ; **SAUER JL** ; **WEISSHAAR CL et al.** Gender differences in bicycle saddle pressure distribution during seated cycling. *Med Sci Sports Exerc*, 2008, vol. 40, 1126-1134 **[0352]**
- **GUESS MK** ; **PARTIN SN** ; **SCHRADER S et al.** Women's bike seats: a pressing matter for competitive female cyclists. *J Sex Med*, 2011, vol. 8, 3144-53 **[0352]**
- **BRESSEL E** ; **BLISS S** ; **CRONIN J**. A field-based approach for examining bicycle seat design effects on seat pressure and perceived stability. *Appl Ergon*, 2009, vol. 40, 472-476 **[0352]**
- The Experimental Investigation of Pressure Distribution of the Body Weight on a Road Bike Ergometer with Different Cycling-Pads. **HOFFMANN S.** Master Thesis. Technical University of Munich, 2019 **[0352]**
- **SAUER J** ; **POTTER J** ; **WEISSHAAR C et al.** Influence of gender, power, and hand position on pelvic motion during seated cycling. *Med Sci Sports Exerc*, 2008, vol. 39, 2204-11 **[0352]**
- **CARPES FP** ; **DAGNESE F** ; **KLEINPAUL JF et al.** Bicycle saddle pressure: Effects of trunk position and saddle design on healthy subjects. *Urol Int*, 2009, vol. 82, 8-11 **[0352]**
- **BRAUN-FALCO O** ; **PLEWIG G** ; **WOLFF HH**. Erkrankungen des äußeren weiblichen Genitales. Springer, 1984, 731-736 **[0352]**
- **LEIBOVITCH I** ; **MOR Y**. The vicious cycling: Bicycling related urogenital disorders. *Eur Urol*, 2005, vol. 47, 277-287 **[0352]**
- **JEONG SJ** ; **PARK K** ; **MOON JD et al.** Bicycle saddle shape affects penile blood flow. *Int J Impot Res*, 2002, vol. 14, 513-517 **[0352]**
- **LOWE BD** ; **SCHRADER SM** ; **BREITENSTEIN MJ**. Effect of bicycle saddle designs on the pressure to the perineum of the bicyclist. *Med Sci Sports Exerc*, 2004, vol. 36, 1055-1062 **[0352]**
- **LARSEN AS** ; **LARSEN FG** ; **SORENSEN FF et al.** The effect of saddle nose width and cutout on saddle pressure distribution and perceived discomfort in women during ergometer cycling. *Appl Ergon*, 2018, vol. 70, 175-181 **[0352]**
- **KEYTEL LR** ; **NOAKES TD**. Effects of a novel bicycle saddle on symptoms and comfort in cyclists. *SAMJ S Afr Med J*, 2002, vol. 92, 295-298 **[0352]**
- **BURY K** ; **LEAVY JE** ; **LAN C et al.** A saddle sores among female competitive cyclists: A systematic scoping review. *J Sci Med Sport*, 2021, vol. 24, 357-367 **[0352]**
- **BINI RR** ; **HUNTER JR**. Pain and body position on the bicycle in competitive and recreational road cyclists: A retrospective study. *Sports Biomech*, 2021, 1-14 **[0352]**

- Efficiency of Cycling Pads in Reducing Seat Pressure During Cycling. **DE BRUYNE G** ; **AERTS JM** ; **BERCKMANS D**. Advances in Intelligent Systems and Computing. Springer International Publishing Ag, 2019, vol. 777, 38-47 **[0352]**
- **MARCOLIN G** ; **PANIZZOLO FA** ; **PAOLI A et al.** Experimental methods for the mechanical characterization of cycling short pads. *Proc Inst Mech Eng P J Sport Eng Technol*, 2018, vol. 232, 22-27 **[0352]**
- **RACCUGLIA M** ; **SALES B** ; **HEYDE C et al.** Clothing comfort during physical exercise-determining the critical factors. *Appl Ergon*, 2018, vol. 73, 33-41 **[0352]**
- **MELLION MB**. Common cycling injuries - management and prevention. *Sports Med*, 1991, vol. 11, 52-70 **[0352]**
- **SILBERMAN MR** ; **WEBNER D** ; **COLLINA S et al.** Road bicycle fit. *Clin J Sport Med*, 2005, vol. 15, 271-276 **[0352]**